Contribution of high energy configurations to longitudinal and transverse form factors in **p**- and **sd**-shell nuclei

F. A. Majeed & L. A. Najim

ONLINE FIRST

ISSN: 0973-1458

Indian Journal of Physics

Official Publication of the Indian Association for the Cultivation of Science

Indian Association for the Cultivation of Science

🖘 Springer

🖘 Springer

Springer

IJP

ORIGINAL PAPER

Contribution of high energy configurations to longitudinal and transverse form factors in *p*- and *sd*-shell nuclei

F A Majeed[1]* and L A Najim[2]

[1]Department of Physics, College of Education for Pure Sciences, University of Babylon, PO Box 4, Hilla, Babylon, Iraq

[2]Department of Physics, College of Science, University of Mosul, Mosul, Iraq

Abstract: Longitudinal and transverse electron scattering form factors for some selected positive and negative parity states of stable odd-A nuclei (^{7}Li, ^{13}C and ^{17}O) in the *p*- and *sd*-shells are investigated by considering the higher energy configurations outside the *p*- and *sd*-shells. The higher energy configurations, referred to as core polarization effects, are considered by means of a microscopic theory that includes excitations from the core 1*s*-1*p*, 2*s*-1*d* orbits to the higher allowed orbits with $4\hbar\omega$ excitations. The calculations are performed in the *p*- and *sd*-shell model spaces by employing Cohen-Kurath, Reehal and Wildenthal interactions respectively, while the core polarization effects are calculated with the modified surface delta interaction as residual interaction. The predicted form factors are compared with the available experimental data and it is shown that the inclusion of the higher excited configurations is very essential in the calculations of the form factors and the reduced transition probabilities to obtain reasonable description of the data with no adjustable parameters.

1. Introduction

The fundamental goal of nuclear structure theory is to understand the properties of complex nuclei in terms of the nucleon–nucleon (N–N) interaction [1]. The conventional multi-particle shell model with configuration mixing has proved to be of great practical value in the interpretation of a large number of experimental data such as static properties, but it is not satisfactory to describe the inelastic electron scattering data. In fact, one needs to include the effects of higher configurations outside the *p*- and *sd*-shell model space, called core-polarization (CP) effects. The concept of the CP effects has been introduced in order to account for the participation of configurations from outside of the model space in the transition. The CP effects have been calculated by using microscopic models to study the Coulomb form factors for transition between single-particle (or- hole) states

with *LS* closed shell [2]. The Coulomb form factors for E4 transition in *sd*-shell nuclei have been investigated by Sagawa et al. [3] taking into account core polarization effects using self consistent Hartree-Fock + random phase approximation calculations, which improve their calculations significantly and agree well with the experimental form factors. A microscopic model has recently been used [4, 5] in order to study the CP effects on the longitudinal form factors of *p*- and *fp*-shell nuclei. For *p*-shell nuclei, Cohen and Kurath [6] model explains well the low-energy properties of *p*-shell nuclei. However, at higher-momentum transfer, it fails to describe the form factors. Cichocki et al. [7] have expanded the shell-model space to include $2\hbar\omega$ configurations in describing the form factors of ^{10}B and have found only a 10 % improvement in the calculations of form factors. The effect of CP is considered by Sato et al. [8] to describe the form factors of ^{12}C and ^{13}C. The first-order CP effects have been considered by Sato et al. [9] with the *p*-shell model space and it significantly improves their work in comparison with the experimental data. The work of Radhi et al. [10–14],

*Corresponding author, E-mail: fouadalajeeli@yahoo.com

for nuclei in the beginning of *p*-shell and at the end of *sd*-shell, have proved that the inclusion of the CP effect is very important to be added to the model space calculations of the form factors.

Large-basis no-core-shell model (NCSM) calculations have been performed [15, 16] for *p*-shell nuclei using six major shells (from 1*s* to 3*p*–2*f*–1*h*). Barrett et al. [17] have performed *ab initio* (NCSM) for *p*-shell nuclei for arbitrary nucleon–nucleon (NN) and NN + three-nucleon (NNN) interactions with exact preservation of all symmetries. In these calculations all nucleons are considered as active. However, constrained by computer capabilities, one can use a truncated no-core calculation, where only a few $\hbar\omega$ excitations of the lowest unperturbed configurations are included. As the number of $\hbar\omega$ increases, the result converges and approaches to those of the full no-core calculations [18].

The aim of the present work is to investigate the effect of core polarization on the longitudinal and transverse form factors of several selected positive and negative parity states for *p*-shell (^{7}Li, ^{13}C) and *sd*-shell (^{17}O) nuclei. The one body density matrix (OBDM) element used in the present work have been calculated by using Cohen-Kurath (CK) [6] for *p*-shell and Reehal and Wildenthal [19] for *sd*-shell, by generating the wave functions of a given transition in the known nuclei using the modified version of shell model code Oxbash [20]. The higher-energy configurations outside the model are taken into account as first-order core polarization by means of a microscopic theory, which adds the shell model wave functions and highly excited states. Transitions from the core 1*s*-1*p*, 2*s*-1*d*-shell orbits to all the higher allowed orbits with excitations up to $4\hbar\omega$ are taken into account. The effective charges are not included in the present calculations of the form factors, which have been used by several authors in this mass region [12, 21]. The modified surface delta interaction (MSDI) [22] have been employed as the residual interaction in the CP calculation. The harmonic oscillator (HO) potential with size parameter *b* chosen to reproduce the measured root mean square (rms) charge radii of these nuclei have been used to produce the single-particle wave functions.

2. Theoretical consideration

The core polarization effect on the form factors is based on a microscopic theory, which combines shell model wave functions and configurations with higher energy as first order perturbations; these are called CP effects. The reduced matrix elements of the electron scattering operator T_Λ is expressed in terms of the residual interaction V_{res} as follows: as the sum of the product of the elements of the one-body density matrix (OBDM) $\chi^\Lambda_{\Gamma_f \Gamma_i}(\alpha, \beta)$ times the single-particle matrix elements and is given by

$$\langle \Gamma_f |||T_\Lambda|||\Gamma_i \rangle = \langle \Gamma_f |||T_\Lambda|||\Gamma_i \rangle_{\mathrm{ms}} + \langle \Gamma_f |||\delta T_\Lambda|||\Gamma_i \rangle_{\mathrm{CP}},$$
(1)

where the states $| \Gamma_i \rangle$ and $| \Gamma_f \rangle$ are described by the model space wave functions. Greek symbols are used to denote quantum numbers in coordinate space and isospace, i.e. $\Gamma_i \equiv J_i T_i$, $\Gamma_f \equiv J_f T_f$ and $\Lambda = JT$.

The model space (ms) matrix element is expressed as the sum of the product of the elements of the one-body density matrix (OBDM) $\chi^\Lambda_{\Gamma_f \Gamma_i}(\alpha, \beta)$ times the single-particle matrix elements and is given by [23]

$$\langle \Gamma_f |||T_\Lambda|||\Gamma_i \rangle_{\mathrm{ms}} = \sum_{\alpha,\beta} \chi^\Lambda_{\Gamma_f \Gamma_i}(\alpha, \beta)\langle \alpha |||T_\Lambda|||\beta \rangle,$$
(2)

where α and β denote labels for single-particle states (isospin is included) for the model space.

Similarly, the higher-energy configurations (CP) matrix element is written as

$$\langle \Gamma_f |||\delta T_\Lambda|||\Gamma_i \rangle_{\mathrm{CP}} = \sum_{\alpha,\beta} \chi^\Lambda_{\Gamma_f \Gamma_i}(\alpha, \beta)\langle \alpha |||\delta T_\Lambda|||\beta \rangle,$$
(3)

$$\langle \alpha |||\delta T_\Lambda|||\beta \rangle = \langle \alpha |||T_\Lambda \frac{Q}{E_i - H_0} V_{res}|||\beta \rangle$$
$$+ \langle \alpha |||V_{res} \frac{Q}{E_f - H_0} T_\Lambda|||\beta \rangle.$$
(4)

The operator Q is the projection operator onto the space outside the model space. For the residual interaction, V_{res}, we adopt the MSDI [22]. E_i and E_f are the energies of the initial and final states, respectively. The CP terms are written as [22]

$$\langle \alpha |||\delta T_\Lambda|||\beta \rangle = \sum_{\alpha_1,\alpha_2,\Gamma} \frac{(-1)^{\beta+\alpha_2+\Gamma}}{e_\beta - e_\alpha - e_{\alpha_1} + e_{\alpha_2}}(2\Gamma + 1)$$
$$\times \begin{Bmatrix} \alpha & \beta & \Lambda \\ \alpha_2 & \alpha_1 & \Gamma \end{Bmatrix}\sqrt{(1+\delta_{\alpha_1\alpha})(1+\delta_{\alpha_2\beta})}$$
$$\times \langle \alpha\alpha_1|V_{res}|\beta\alpha_2\rangle\langle \alpha_2|||T_\Lambda|||\alpha_1\rangle$$
$$+ \text{terms with } \alpha_1 \text{ and } \alpha_2 \text{ exchanged with}$$
$$\text{an overall minus sign}$$
(5)

where the index α_1 and α_2 runs over particles states and *e* is the single-particle energy. The CP parts are calculated by keeping the intermediate states up to the 2*p*1*f*-shells. The single-particle matrix element reduced in both spin and isospin is written in terms of the single-particle matrix element reduced in spin only [22].

$$\langle \alpha_2|||T_\Lambda|||\alpha_1\rangle = \sqrt{\frac{2T+1}{2}}\sum_{t_z} I_T(t_z)\langle \alpha_2||T_\Lambda||\alpha_1\rangle$$
(6)

with

$$I_T(t_z) = \begin{cases} 1, & \text{for } T=0, \\ (-1)^{1/2-t_z}, & \text{for } T=1, \end{cases}$$

where $t_z = 1/2$ for protons and $-1/2$ for neutrons. The reduced single-particle matrix element of the Coulomb operator is given by [24]

$$\langle \alpha_2 || T_J || \alpha_1 \rangle = \int_0^\infty dr\, r^2 j_J(qr) \langle \alpha_2 || Y_J || \alpha_1 \rangle R_{n_1 \ell_1} R_{n_2 \ell_2} \qquad (7)$$

where $j_J(qr)$ is the spherical Bessel function and $R_{n\ell}(r)$ is the single-particle wave function.

The electron scattering form factor involving angular momentum J and momentum transfer q, between the initial and final nuclear shell model states of spin $J_{i,f}$ and isospin $T_{i,f}$ is [25]

$$|F_J(q)|^2 = \frac{4\pi}{Z^2(2J_i+1)} \left| \sum_{T=0,1} \begin{pmatrix} T_f & T & T_i \\ -T_z & 0 & T_z \end{pmatrix} \right|^2$$
$$\times |\langle \alpha_2 ||| T_\Lambda ||| \alpha_1 \rangle|^2 |F_{c.m}(q)|^2 \; |F_{f.s}(q)|^2 \qquad (8)$$

where T_z is the projection along the z-axis of the initial and final isospin states and is given by $T_z = (Z-N)/2$. The nucleon finite-size (f.s) form factor is $F_{f.s}(q) = \exp(-0.43q^2/4)$ and $F_{c.m}(q) = \exp(q^2 b^2/4A)$ is the correction for the lack of translational invariance in the shell model. A is the mass number and b is the harmonic oscillator size parameter.

The electric transition strength is given by [22]

$$B(CJ,k) = \frac{Z^2}{4\pi} \left[\frac{(2J+1)!!}{k^J} \right]^2 F_J^2(k) \qquad (9)$$

where $k = E_x/\hbar c$.

3. Results and discussion

The parameters of the MSDI used in the present calculations of the CP effects are denoted by A_T, B and C [22], where T indicates the isospin (0,1). These parameters are taken as $A_0 = A_1 = B = 25/A$ and $C = 0$, where A is the mass number.

3.1. The ^{7}Li nucleus

The ground state of ^{7}Li is $J_f^\pi T = 3/2^- 1/2$. According to the conventional p-shell model, it is described in terms of three nucleons outside a closed $1s$-shell, with size parameter $b_{rms} = 1.77$ fm obtained from a fit to nuclear charge radius [26].
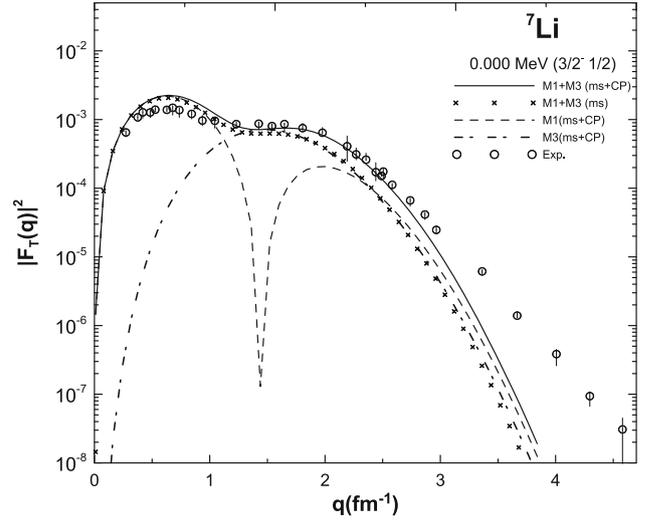

Fig. 1 Transverse magnetic $M1$ and $M3$ form factors for $3/2^- 1/2$ (0.0 MeV) in ^{7}Li. The data are taken from [27]

3.1.1. The 0.000 MeV, $J_f^\pi T = 3/2^- 1/2$ state

Figure 1 shows the calculated transverse magnetic $M1$ and $M3$ form factors for the ground state ($J_f^\pi T = 3/2^- 1/2$) including the CP effects respectively. The multipole decomposition is displayed as indicated by $M1+M3$. The $1p$-shell calculation for the total $M1+M3$ transverse form factors is shown by the cross symbols curve, where the experimental data are overestimated for $q < 1.2\,\text{fm}^{-1}$. The inclusion of the higher excited states enhances the calculation of the total $M1+M3$ transverse form factor as shown by the solid curve, where the experimental data are well described at momentum transfer $1.2 \le q \le 2.6\,\text{fm}^{-1}$. The inclusion of the CP effects enhances the calculations of the transverse $M1 + M3$ form factors by a factor of 2 over the $1p$-shell calculations and brings the total transverse form factor near to the measured data. Our results as well as the results obtained by Lichtenstadt et al. [27] using Woods-Saxon radial wave functions including the meson-exchange currents (MEC) are unable to reproduce the experimental data for $q > 3\,\text{fm}^{-1}$. Calculations using more realistic nucleon wave functions obtained from a well of finite depth, for example, the Woods-Saxon potential leads to an effective decrease of the form factor for high q values [28]. This problem still needs more investigation from the microscopic point of view.

3.1.2. The 0.478 MeV, $J_f^\pi T = 1/2^- 1/2$ state

Figure 2 presents the calculations of the transverse $M1$ and $E2$ form factors and their multipole decomposition $M1 + E2$ for the state $J_f^\pi T = 1/2^- 1/2$ at 0.478 MeV. The dashed and dash-dotted curves represents the transverse $M1$ and
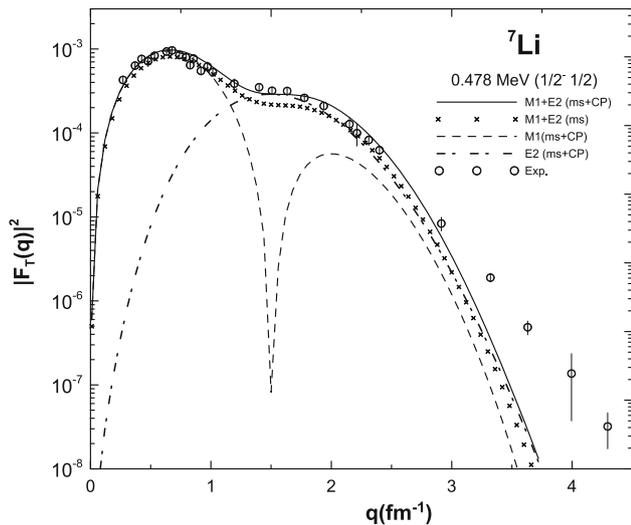
Fig. 2 Transverse magnetic $M1$ and electric $E2$ form factors for $1/2^-1/2$ (0.478 MeV) in ^{7}Li. The data are taken from [27]

$E2$ form factors calculated including the CP effects respectively. The cross symbols curve represents the transverse $M1 + E2$ without the CP effects. The inclusion of the higher excited states improves the transverse $M1 + E2$ form factors and reproduce the data very well up to $q \leq 3\,\text{fm}^{-1}$ as shown by the solid curve. The calculations including the CP effects fail to describe the data at high momentum transfer at $q > 3\,\text{fm}^{-1}$, similar to the results obtained by Lichtenstadt et al. [27] by using the Woods–Saxon radial wave functions and meson exchange currents (MEC).

3.1.3. The 0.478 MeV, $J_f^\pi T = 1/2^- 1/2$ state

The harmonic oscillator HO single-particle wave functions employed with size parameter $b = 1.77$ fm are chosen to reproduce the nuclear charge radius [26]. Figure 3 presents the calculation of the longitudinal $C2$ form factor, where the model space calculations shown by the dashed curve are unable to reproduce the measured data and underestimate by a factor of 2.8 and the $B(C2 \uparrow)$ value by a factor of 5 as displayed in Table 1. The results of the core polarization (CP) effects are shown by the dash-dotted curve. The calculations including the CP effects as shown by the solid curve are in excellent agreement up to momentum transfer of 3 fm^{-1} and at q around 3.3 fm^{-1} the measured longitudinal form factor shows a diffractive structure. Our calculations as well as all previous calculations [10, 21, 29, 30] fail to reproduce these structures in all model spaces. Booten and Van Hees [31] have included meson exchange currents (MEC) in their $1p$-shell calculations predicted second minimum at $q \approx 3.2\,\text{fm}^{-1}$ in their analysis for the $M1$ transition of the ground state in ^{6}Li. Radhi et al. [10] have concluded that there is no conclusive evidence for the explanation of the structures in the
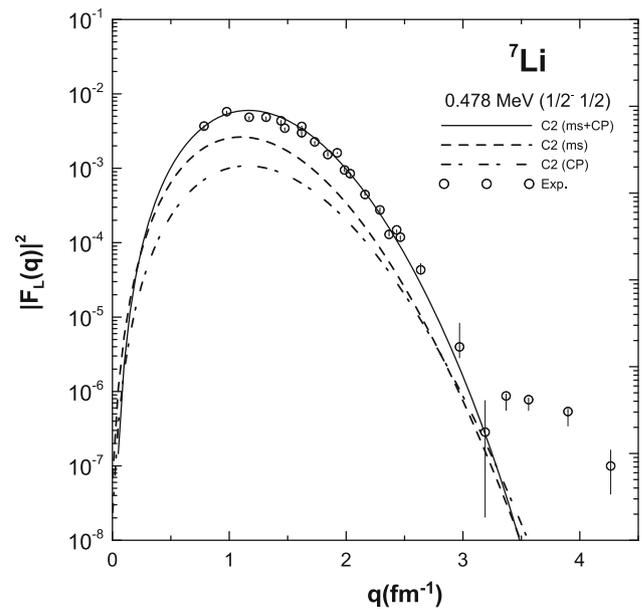

Fig. 3 Longitudinal $C2$ form factor for $1/2^-1/2$ (0.478 MeV) in ^{7}Li. The data are taken from [27]

longitudinal form factors of ^{7}Li. The inclusion of the CP effects enhances the calculations of the form factors as well as the $B(C2 \uparrow)$ in which, model space predicts 1.785 $e^2\,\text{fm}^4$, which underestimates the observed value $8.3 \pm 0.5\,e^2\,\text{fm}^4$ [32] by about 78 % and with the inclusion of the CP effects the predicted value is 6.845 $e^2\,\text{fm}^4$, which also underestimates the measured value by about 17.5 % with improvement by a factor of ~ 4 over the model space calculations and more closer to the measured value than the value calculated by Radhi et al. [10] as tabulated in Table 1.

3.2. The ^{13}C nucleus

According to the conventional shell model, this nucleus is described by taking the core at ^{4}He with nine valence nucleons distributed over ($1p_{3/2}, 1p_{1/2}$) orbits. The single-particle radial wave functions used are those of harmonic oscillator potential with size parameter brms = 1.64 fm [33] to match the measured root mean square radius of ^{13}C.

3.2.1. The 3.68 MeV, $J_f^\pi T = 3/2_1^- 1/2$ state

Figure 4 shows a comparison of the calculated transverse $M1$ and $E2$ form factors as dashed and dash-dotted curves respectively, where CP effects are included. The multipole decomposition $M1 + E2$ including the CP effects are shown by the solid curve, where the data are reasonably described. The peak value for the total $M1 + E2$ is found at $q \approx 0.7\,\text{fm}^{-1}$ in the present work, while those calculated by Millener et al. [33] is found at $q \approx 0.5\,\text{fm}^{-1}$ by using the Woods-Saxon potential, where they have normalized the
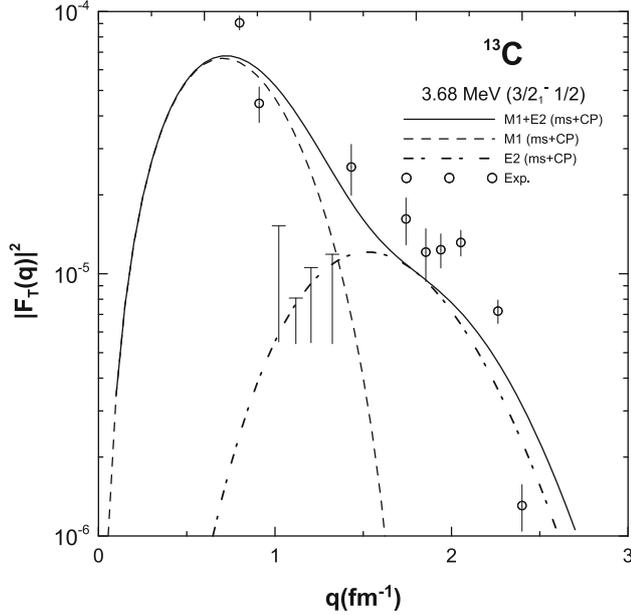
Fig. 4 Transverse magnetic $M1$ and electric $E2$ form factors for $3/2_1^- 1/2$ (3.68 MeV) in ^{13}C. The data are taken from [33]
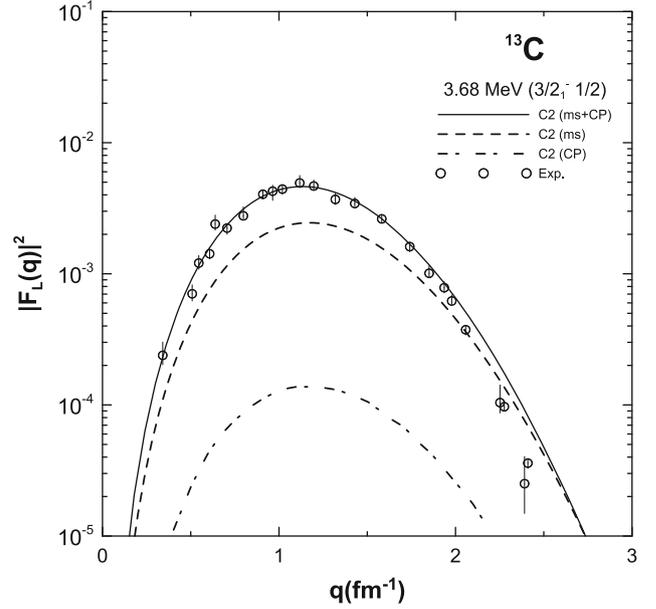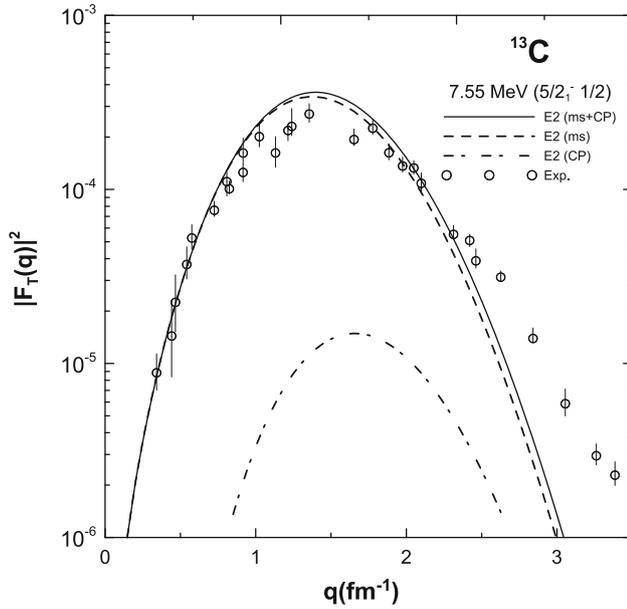

Fig. 5 Transverse $E2$ for factor for $5/2_1^- 1/2$ (7.55 MeV) in ^{13}C. The data are taken from [33]

$M1$ form factor by a factor of 0.53 to reproduce the experimental $B(M1)$ value. The core polarization effects added to the model space calculations shift the peak position toward higher momentum transfer.

3.2.2. The 7.55 MeV, $J_f^\pi T = 5/2_1^- 1/2$ state

The transverse $E2$ form factor for the state $J_f^\pi T = 5/2^+ 1/2$ at $E_x = 7.55$ MeV is shown by the solid line in Fig. 5 including

Fig. 6 Longitudinal $C2$ form factor of $3/2_1^- 1/2$ (3.68 MeV) in ^{13}C. The data are taken from [33]

the CP effects in which, the experimental data are well described at $q \leq 1.0 \, \mathrm{fm}^{-1}$. The dashed and the dash-dotted curves represents the $1p$-shell calculations and the CP calculations respectively. The $1p$-shell calculations as well as the $1P+CP$ calculations overshoot the experimental data for the momentum transfer region $q \sim 1.1 - 2.1 \, \mathrm{fm}^{-1}$. Our results as well as the results obtained by Millener et al. [33] using Woods-Saxon wave functions are unable to reproduce the transverse $E2$ form factor for $q \geq 2.5 \, \mathrm{fm}^{-1}$.

3.2.3. The 3.68 MeV, $J_f^\pi T = 3/2_1^- 1/2$ state

The model space calculations underestimate the experiment as presented by the dashed curve as shown in Fig. 6. The results of the CP effects are shown by dash-dotted curve. The inclusion of the CP effects as shown by the solid line enhances the calculations of the $C2$ form factor appreciably and reproduce the experimental data very well up to momentum transfer $q \leq 2.1 \, \mathrm{fm}^{-1}$. $B(C2 \uparrow)$ calculated with the model space is found to be $6.88 \, e^2 \, \mathrm{fm}^4$ in comparison with the measured value of $12.92 \pm 0.55 \, e^2 \, \mathrm{fm}^4$ [33]. The calculated $B(C2 \uparrow)$ including the CP effects predicts the value of $11.02 \, e^2 \, \mathrm{fm}^4$ with improvement by a factor of 1.6 over the model space calculations and are in better agreement than the value calculated by Radhi et al. [10] by a factor of 0.99 in comparison with the observed value as displayed in Table 1.

3.2.4. The 9.90 MeV, $J_f^\pi T = 3/2_2^- 1/2$ state

The longitudinal $C2$ form factor are calculated with and without the inclusion of the CP effects as shown by the
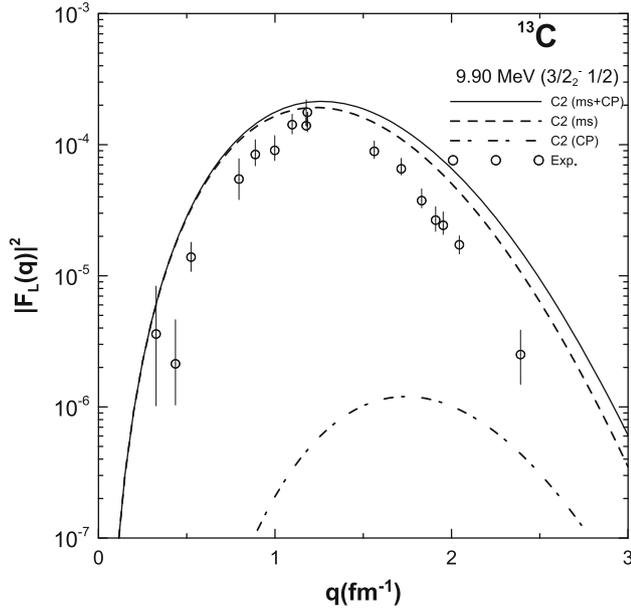
Fig. 7 Longitudinal $C2$ form factor of $3/2_2^- 1/2$ (9.90 MeV) in ^{13}C. The data are taken from [33]

Fig. 8 Longitudinal $C2$ form factor of $1/2_1^+ 1/2$ (0.87 MeV) in ^{17}O. The data are taken from [34]

solid and and dashed curves respectively while the dash-dotted curve represents the CP results as shown in Fig. 7. The model space as well as the (ms + CP) calculations fail to reproduce the experimental data in all momentum transfer regions.

3.3. ^{17}O nucleus

According to the conventional sd-shell model, this nucleus is described by a single neutron distributed over the $1d_{5/2}$, $2s_{1/2}$ and $1d_{3/2}$ outside a closed ^{16}O core. In the present work the core is taken at ^{12}C with five active nucleons distributed over $1p_{1/2}$, $1d_{5/2}$, $2s_{1/2}$ and $1d_{3/2}$ active orbits. The oscillator parameter b is taken to be 1.678 fm to reproduce the rms charge radius [34, 35].

3.3.1. The 0.87 MeV, $J_f^\pi T = 1/2_1^+ 1/2$ state

Figure 8 shows the $C2$ form factor, where the solid curve corresponds to the model space plus the CP effects, the dashed curve represents the model space calculations only
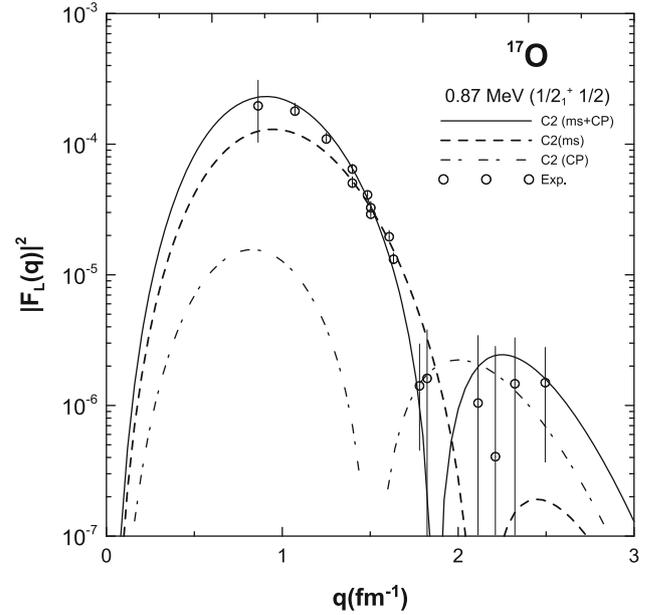
and the dash-dotted curve are the calculations of the core polarization. The model space calculations underestimate the measured $C2$ form factor and unable to locate the diffraction minimum. The inclusion of the CP effects enhances the calculations and describes the data very well at both first and second maxima and locate the diffraction minimum at its right position. Our results and the results obtained by Radhi et al. [36] are the same for the first maxima and are in better agreement with the experiment than those obtained by Horikawa et al. [2] using the attractive triplet-odd interaction (ATO). The model space predicts the value of $B(C2 \uparrow)$ to be zero in comparison with the measured value at $2.18 \pm 0.16 \, e^2 \, \text{fm}^4$ [34]. The inclusion of the CP effects reproduced the measured $B(C2 \uparrow)$ value correctly, as displayed in Table 1.

3.3.2. The 5.09 MeV, $J_f^\pi T = 3/2_1^+ 1/2$ state

The longitudinal $C2$ and $C4$ form factors represented by the dashed and dash-dotted curves respectively are calculated with the inclusion of the CP effects as shown in

Table 1 Theoretical values of the reduced transition probabilities $B(C2 \uparrow, k)$ (in units of $e^2 \, \text{fm}^4$) and in comparison with experimental values and other theoretical calculations

Nucleus	J_f^π	T_f	E_x (MeV)	b (fm)	ms	ms+CP	Other	Exp.
^{7}Li	$1/2^-$	1/2	0.478	1.77[a]	1.785	6.845	6.507[b]	8.3 ± 0.5[c]
^{13}C	$3/2_1^-$	1/2	3.68	1.64[d]	6.88	11.02	10.94[b]	12.92 ± 0.55[d]
^{17}O	$1/2_1^+$	1/2	0.889	1.678[e]	0.0	2.09	2.02[b]	2.18 ± 0.16[f]
^{17}O	$3/2_1^+$	1/2	5.09	1.678[e]	0.0	2.0		2.05 ± 0.20[f]

[a] Ref. [26], [b] Ref. [10], [c] Ref. [32], [d] Ref. [33], [e] Ref. [35], [f] Ref. [34]
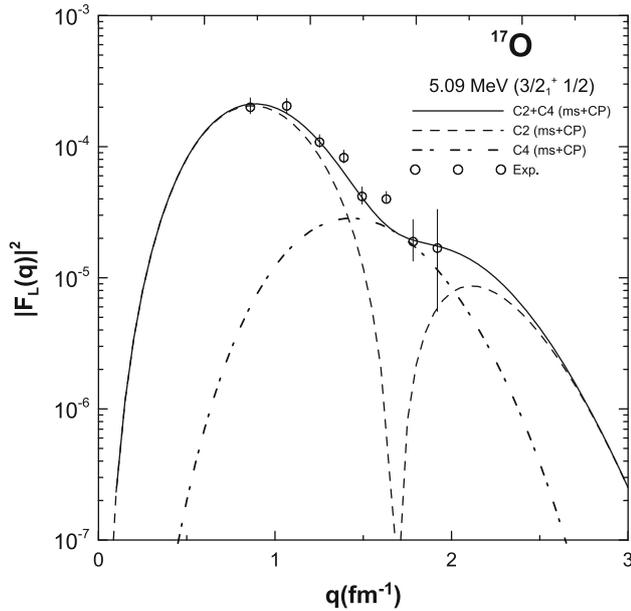
Fig. 9 Longitudinal $C2$ and $C4$ form factors of $3/2_1^+1/2$ (5.09 MeV) in ^{17}O. The data are taken from [34]

Fig. 10 Transverse $M3$ form factor $1/2_1^+1/2$ (0.87 MeV) in ^{17}O. The data are taken from [34]

Fig. 9. The solid curves are the multipole decomposition $C2 + C4$, which are able to reproduce the data very well in the range $q \approx 0.86-1.92$ fm^{-1}. Our calculations agree with the calculations made by Manley et al. [34], where they have used weak-coupling model with an oscillator parameter $b = 1.779 \pm 0.016$ fm. The model space calculations for $B(C2\uparrow)$ gives zero value in comparison with the measured value of $2.05 \pm 0.20\, e^2$ fm^4 [34] and the inclusion of the CP effects predicts the value $2.0\, e^2$ fm^4, which is correctly reproduced.

3.3.3. ^{17}The 0.87 MeV, $J_f^\pi T = 1/2_1^+ 1/2$ state

Figure 10 presents the transverse $M3$ form factor for the $J_f^\pi T = 1/2_1^+1/2$ state. The inclusion of the CP effects succeeded in describing the measured form factor in all momentum transfer regions and the location of the diffraction minimum are correctly reproduced. Our results are similar to those calculated by Manley et al. [34] using the weak-coupling model with an oscillator parameter $b = 1.779 \pm 0.016$ fm.

4. Conclusions

The inclusion of the CP effects are found to be very essential in the calculations of the longitudinal and transverse form factors and gives remarkably good agreement over the model space calculations for the form factors and the absolute strengths. The calculations with $(0 + 2 + 4)\hbar\omega$ gives 96 % of the matrix element. The $1p$-shell and sd-shell
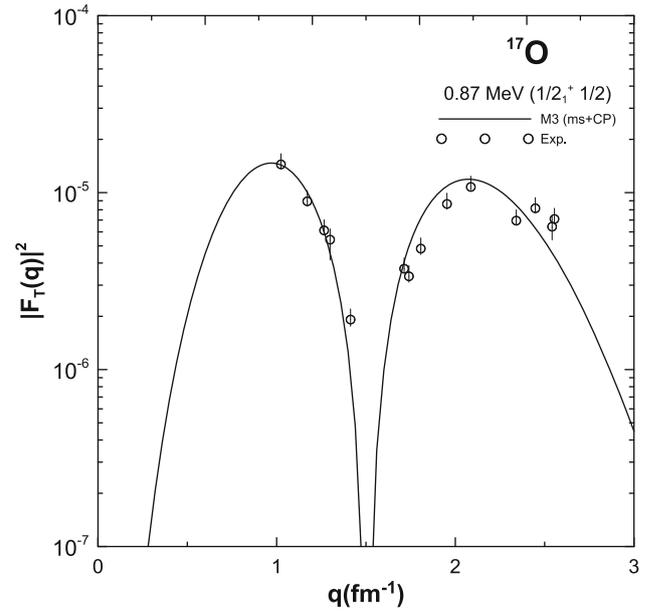
models are able to predict the static properties and energy levels of nuclei lies in the $1p$ and sd-shell regions but it can not describe the dynamic properties such as $C2$ transition rates and electron scattering form factors. The choice of MSDI as residual effective interaction for core polarization calculations is adequate. The inclusion of higher-excited configurations by means of CP enhances the form factors and brings the theoretical results closer to the experimental data. These calculations can be extended to study more nuclei in this mass region.

References

[1] J A Pinston and J Genevey *J. Phys G: Nucl. Part. Phys.* **30** R57 (2004)
[2] Y Horikawa, T Hoshino and A Arima *Nucl. Phys. A* **278** 297 (1977)
[3] H Sagawa and B A Brown *Nucl. Phys. A* **430** 84 (1984)
[4] F A Majeed *Phys. Scr.* **85** 065201 (2012)
[5] F A Majeed and F M Hussain *Rom. Journ. Phys.* **59** 95 (2014)
[6] S Cohen and D Kurath *Nucl. Phys.* **73** 1 (1965)
[7] A Cichocki et al. *Phys. Rev. C* **51** 2406 (1995)
[8] T Sato, K Koshigiri and H Ohtsubo *Z. Phys. A* **320** 507 (1985)
[9] T Sato, N Odagawa, H Ohtsubo and T S H Lee *Phys. Rev. C* **49** 776 (1994)
[10] R A Radhi, A A Abdullah, Z A Dakhil and N M Adeeb *Nucl. Phys. A* **696** 442 (2001)
[11] R A Radhi *Nucl. Phys. A* **707** 56 (2002)
[12] R A Radhi *Eur. Phys. J. A* **16** 381 (2003)
[13] R A Radhi *Nucl. Phys. A* **716** 100 (2002)

[14] R A Radhi, A A Abdullah and A H Raheem *Nucl. Phys. A* **798** 16 (2008)

[15] D C Zheng, J Vary and B R Barrett *Phys. Rev. C* **50** 2841 (1994)

[16] D C Zheng, B R Barrett, J P Vary and W C Haxton *Phys. Rev C* **52** 2488 (1995)

[17] B R Barrett, P Navratil and J P Vary *Prog. Part. Nucl. Phys.* **69** 131 (2013)

[18] R A Radhi, N M Adeeb and A K Hashim *J. Phys. G: Nucl. Part. Phys.* **36** 105102 (2009)

[19] B S Reehal and B H Wildenthal *Part. Nucl.* **6** 137 (1973)

[20] B A Brown et al. MSUNSCL Report No. 1289 (2004)

[21] S Karataklidis, B A Brown, K Amos and P J Dortmans *Phys. Rev. C* **55** 2826 (1997)

[22] P J Brussaard and P W M Glaudemans *Shell-Model Applications in Nuclear Spectrscopy* (Amsterdam: North Holland) (1977)

[23] B A Brown, R Radhi and B H Wildenthal *Phys. Rep.* **101** 313 (1983)

[24] T de Forest Jr and J D Walecka *Adv. Phys.* **15** 1 (1966)

[25] T W Donnelly and I Sick *Rev. Mod. Phys.* **56** 461 (1984)

[26] H de Vries, C W de Jager and C de Vries *At. Data Nucl. Data Tables* **36** 500 (1987)

[27] J Lichtenstadt et al. *Phys. Lett. B* **219** 394 (1989)

[28] L Clausen, R J Peterson and R A Lindgren *Phys. Rev. C* **38** 589 (1988)

[29] M Unkelbach and H M Hofmann *Phys. Lett. B* **261** 211 (1991)

[30] J G L Booten, A G M van Hees, P W M Glaudemans and P J Brussaard *Nucl. Phys. A* **549** 197 (1992)

[31] J G L Booten and A G M van Hees *Nucl. Phys. A* **569** 510 (1994)

[32] R Yen, L S Cardman, D Kalinsky, J R Legg and C K Bockelman *Nucl. Phys. A* **235** 135 (1974)

[33] D J Millener et al. *Phys. Rev. C* **39** 14 (1989)

[34] D M Manley et al. *Phys. Rev C* **36** 1700 (1987)

[35] C W De Jager, H De Vries and C De Vries *At. Data Nucl. Data Tables* **14** 179 (1974)

[36] R A Radhi *Eur. Phys. J. A* **16** 387 (2003)